Inorg. Chem. **2009**, *48*, 4179−4189

Synthesis of Cyclometallated Platinum Complexes with Substituted Thienylpyridines and Detailed Characterization of Their Luminescence Properties

Dmitry N. Kozhevnikov,*,†,‡ Valery N. Kozhevnikov,*,§ Maria M. Ustinova,‡,|| Amedeo Santoro,§ Duncan W. Bruce,*,§ Burkhard Koenig,|| Rafał Czerwieniec,⊥ Tobias Fischer,⊥ Manfred Zabel,⊥ and Hartmut Yersin*,⊥

Institute of Organic Synthesis, Ural Branch of Russian Academy of Sciences, Kovalevskoy 22, Ekaterinburg, 620219, Russia, Ural State Technical University, Mira 19, Ekaterinburg, 620002, Russia, Department of Chemistry, University of York, Heslington, York YO10 5DD, U.K., Institute of Organic Chemistry and Institute of Physical and Theoretical Chemistry, University of Regensburg, Universitätsstrasse 31, D-93053 Regensburg, Germany

Received December 19, 2008

Synthesis of various derivatives of 2-(2-thienyl)pyridine via substituted 3-thienyl-1,2,4-triazines is reported. The final step of the synthesis is a transformation of the triazine ring to pyridine in an aza-Diels−Alder-type reaction. The resulting 5-aryl-2-(2-thienyl)pyridines (HL1-HL4) and 5-aryl-2-(2-thienyl)cyclopenteno[*c*]pyridines (HL5-HL8) (with aryl = phenyl, 4-methoxyphenyl, 2-naphtyl, and 2-thienyl) were used as cyclometallating ligands to prepare a series of eight luminescent platinum complexes of the type [Pt(L)(acac)] (L = cyclometallating ligand, acac = acetylacetonato). X-ray single crystal structures of three complexes of that series, [Pt(L5)(acac)] = [Pt(5-phenyl-2-(2-thienyl)cyclopenteno[*c*]pyridine)(acac)], [Pt(L6)(acac)] = [Pt(5-(4-methoxy)-2-(2-thienyl)cyclopenteno[*c*]pyridine)(acac)], and [Pt(L7)(acac)] = [Pt(5-(2-naphtyl)-2-(2-thienyl) cyclopenteno[*c*]pyridine)(acac)] were determined. Photoluminescence and electronic absorption spectra of the new [Pt(L)(acac)] complexes are reported. For two representative compounds of that series, [Pt(L4)(acac)] and [Pt(L5)(acac)], a detailed photophysical characterization based on highly resolved emission and excitation spectra, as well as on emission decay properties, was carried out. The studies down to low temperature (T = 1.2 K) and up to high magnetic fields (B = 10 T) allowed us to characterize the three individual substates of the emitting triplet state. In particular, it is shown that the lowest triplet states of [Pt(L4)(acac)] and [Pt(L5)(acac)] are largely ligand-centered (LC) of $^3\pi\pi^*$ character, which experience only weak spin−orbit couplings to higher lying singlet states.

1. Introduction

During the last two decades, research in the field of the third-row transition metal complexes has gained additional momentum since they were found to be important for a wide range of applications, such as optical chemosensors,[1−4] photocatalysts,[5−7] solar cells,[8−11] biological labels,[12−14] and, in particular, as electroluminescent emitters in organic light

* To whom correspondence should be addressed. E-mail: dnk@ios.uran.ru (D.N.K.), db519@york.ac.uk (D.B.), hartmut.yersin@chemie.uni-regensburg.de (H.Y.).
† Ural Branch of Russian Academy of Sciences.
‡ Ural State Technical University.
§ University of York.
|| Institute of Organic Chemistry, University of Regensburg.
⊥ Institute of Physical and Theoretical Chemistry, University of Regensburg.

(1) Tang, W. S.; Lu, X.-X.; Wong, K. M.-C.; Yam, V. W.-W. *J. Mater. Chem.* **2005**, *15*, 2714–2720.
(2) Chen, H.; Zhao, Q.; Wu, Y.; Li, F.; Yang, H.; Yi, T.; Huang, C. *Inorg. Chem.* **2007**, *46*, 11075–11081.
(3) Demas, J. N.; DeGraff, B. A. *Coord. Chem. Rev.* **2001**, *211*, 317–351.
(4) Zhao, Q.; Cao, T.; Li, F.; Li, X.; Jing, H.; Yi, T.; Huang, C. *Organometallics* **2007**, *26*, 2077–2081.
(5) Belmore, K. A.; Vanderpool, R. A.; Tsai, J. C.; Khan, M. A.; Nicholas, K. M. *J. Am. Chem. Soc.* **1988**, *110*, 2004–2005.
(6) Maruyama, T.; Yamamoto, T. *J. Phys. Chem. B* **1997**, *101*, 3806–3810.
(7) Hissler, M.; McGarrah, J. E.; Connick, W. B.; Geiger, D. K.; Cummings, S. D.; Eisenberg, R. *Coord. Chem. Rev.* **2000**, *208*, 115–137.
(8) Tse, C. W.; Man, K. Y. K.; Cheng, K. W.; Mak, C. S. K.; Chan, W. K.; Liu, Z. T.; Yip, C. T.; Djurišic, A. B. *Chem.—Eur. J.* **2007**, *13*, 328–335.

10.1021/ic802401j CCC: $40.75
Published on Web 04/01/2009

emitting diodes[15−19] (OLEDs). As metal-induced spin−orbit coupling often allows effective singlet−triplet mixing, complexes displaying high photoluminescence (phosphorescence) quantum yields and relatively short emission decay times can be engineered. Such triplet emitters represent attractive candidate materials for conversion of electric energy into light. Cyclometallated platinum complexes incorporating 1,3-diketonates (e.g., acetylacetonato, acac) as spectator ligands were reported to be strongly emissive at room temperature.[19,20] In particular, chemical modification of the chromophoric cyclometallating ligand should enable tuning of emitting properties. On the other hand, specific substitutions may be used for binding of the metal complex to polymers or biomolecules, which results in new applications.

It is known from textbooks that 1,2,4-triazines can be converted into pyridines through an aza-Diels−Alder reaction.[21] Consequently, any synthetic method that creates 1,2,4-triazines can be considered as a method for the synthesis of substituted pyridines. This general idea has been exploited for decades, and a great variety of interesting examples have been described.[22−24] In 1998, Sauer and co-workers applied such an approach specifically for the synthesis of polypyridine ligands and demonstrated how useful this methodology can be in preparing ligands for use in coordination chemistry.[25] Many other examples followed, and the methodology evolved considerably, making functionalized polypyridine ligands readily accessible.[26−31] Thus, a combination of the wide variety of methods for the synthesis of substituted 1,2,4-triazines, coupled with the aza-Diels−Alder reaction with various dienophiles, allows for the synthesis of different functionalized pyridines. In this report, we describe the application of 1,2,4-triazine chemistry to develop a new, efficient, flexible, and straightforward methodology for the synthesis of ligands capable of forming cyclometallated transition metal complexes. For thienylpyridines, we demonstrate how this methodology can be used for fine-tuning photophysical properties of [Pt(L)(acac)] complexes, wherein L is a substituted 2-(2-thienyl)pyridine ligand. Two representatives of this series are studied in more detail to obtain a deeper insight into the nature of the emitting triplet states. This is carried out on the basis of highly resolved emission and excitation spectra, emission decay behavior at a low temperature and under application of high magnetic fields. For these investigations the Shpol'skii matrix isolation technique (the complexes are dissolved in *n*-octane) is applied. These studies allow us to characterize the orbital origin of the lowest triplet state, the individual triplet substates, as well as the importance of spin−orbit coupling (SOC). In particular, this latter property largely determines the luminescence behavior of the studied compounds.

2. Experimental Section

2.1. Equipment. Spectroscopic Methods. Nuclear magnetic resonance spectra were recorded on a Jeol JNM-EX 270 FT NMR system at 270 MHz for ^{1}H and 68 MHz for ^{13}C. Microanalyses were performed using Carlo Erba 1108 Elemental Analyzer controlled with CE Eager 200 software. Mass spectra were done using Varian CH-5 (EI), Finnigan MAT 95 (CI; FAB and FD) or Finnigan MAT TSQ 7000 (ESI) spectrometers. For measurements of UV−vis absorption spectra a Varian Cary 300 double beam spectrometer was used. Luminescence spectra at 300 and 77 K were recorded with a steady-state fluorescence spectrometer (Jobin Yvon Fluorolog 3). Emission decay measurements at 300 and 77 K were performed with a pulsed diode laser (PicoQuant GmbH Model LDH−P-C-375, $\lambda_{exc} = 372$ nm, pulse width 100 ps), attached to the Fluorolog 3 spectrophotometer. For measurements of the luminescence quantum yield an integrating sphere purchased from Labsphere (model 4P-GPS-033-SL with Spectralon inner surface coating) was used. The solutions for room-temperature measurements were degassed by the freeze−pump−thaw technique. The [Pt(L)(acac)] doped poly(methyl metacrylate) (PMMA) thin films were prepared by spin-coating of dichloromethane solutions containing PMMA and the respective [Pt(L)(acac)] complex onto a quartz substrate. Experiments at temperatures below 4.2 K were carried out in a bath cryostat. Temperature was reduced by pumping off the helium vapor. For magnetic field experiments, an Oxford Instruments MD10 cryostat equipped with a 12 T magnet was used. A UV diode laser (Toptica IBeam, 375 nm) was applied as source for non-selective excitation. For site-selective excitation, a pulsed dye laser (Lambdaphysik FL2000, Lambdaphysik Scanmate 2C) was applied using Coumarin 153 and a mixture of Rhodamine B and Rhodamine 6G, respectively. The spectra were recorded with a cooled photomultiplier (RCA C7164R), attached to a Spex 1404

(9) Wong, W.-Y.; Wang, X.-Z.; He, Z.; Djurišić, A. B.; Yip, C.-T.; Cheung, K.-Y.; Wang, H.; Mak, C. S. K.; Chan, W.-K. *Nature Mater.* **2007**, *6*, 521–527.
(10) Polo, A. S. P.; Itokazu, M. K.; Iha, N. Y. M. *Coord. Chem. Rev.* **2004**, *248*, 1343–1361.
(11) Robertson, N. *Angew. Chem., Int. Ed.* **2006**, *45*, 2338–2345.
(12) Peyratout, C. S.; Aldridge, T. K.; Crites, D. K.; McMillin, D. R. *Inorg. Chem.* **1995**, *34*, 4484–4489.
(13) Lo, K. K. W.; Chan, J. S. W.; Lui, L. H.; Chung, C. K. *Organometallics* **2004**, *23*, 3108–3116.
(14) Lo, K. K. W.; Hui, W. K.; Chung, C. K.; Tsang, K. H. K.; Ng, D. C. M.; Zhu, N.; Cheung, K. K. *Coord. Chem. Rev.* **2005**, *249*, 1434–1450.
(15) *Highly Efficient OLEDs with Phosphorescent Materials*; Yersin, H., Ed; Wiley-VCH: Weinheim, 2008.
(16) Cocchi, M.; Kalinowski, J.; Virgili, D.; Williams, J. A. G. *Appl. Phys. Lett.* **2008**, *92*, 113302–113304.
(17) Baldo, M. A.; Thompson, M. E.; Forrest, S. R. *Nature* **2000**, *403*, 750–752.
(18) Tamayo, A. B.; Garon, S.; Sajoto, T.; Djurovich, P. I.; Tsyba, I.; Bau, R.; Thompson, M. E. *Inorg. Chem.* **2005**, *44*, 8723–8732.
(19) Brooks, J.; Babayan, Y.; Lamansky, S.; Djurovich, P. I.; Tsyba, I.; Bau, R.; Thompson, M. E. *Inorg. Chem.* **2002**, *41*, 3055–3066.
(20) Williams, J. A. G. *Top. Curr. Chem.* **2007**, *281*, 205–268.
(21) Joule, J. A.; Mills, K. *Heterocyclic Chemistry*; Blackwell Science Limited: Oxford, 2000; Chapter 5.15.
(22) Neunhoeffer, H. In: *Comprehensive Heterocyclic Chemistry II 6*; Katrizky, A. R., Rees, C. W., Scriven, E. F. V., Eds.; Pergamon Press: Oxford, 1996; pp 50−574.
(23) Boger, D. L.; Panek, J. S. *J. Am. Chem. Soc.* **1985**, *107*, 5745–5754.
(24) Fernandez-Sainz, Y.; Raw, A.; Taylor, R. J. K. *J. Org. Chem.* **2005**, *70*, 10086–10095.
(25) Pabst, G. R.; Sauer, J. *Tetrahedron Lett.* **1998**, *39*, 6687–6690.
(26) Sauer, J.; Heldmann, D. K.; Pabst, G. R. *Eur. J. Org. Chem.* **1999**, 313–321.
(27) Rykowski, A.; Branowska, D.; Kielak, J. *Tetrahedron Lett.* **2000**, *41*, 3657–3658.
(28) Kozhevnikov, V. N.; Kozhevnikov, D. N.; Nikitina, T. V.; Rusinov, V. L.; Chupakhin, O. N.; Zabel, M.; Koenig, B. *J. Org. Chem.* **2003**, *68*, 2882–2888.
(29) Stanforth, S. P.; Tarbit, B.; Watson, M. D. *Tetrahedron Lett.* **2003**, *44*, 693–694.
(30) Kozhevnikov, D. N.; Shabunina, O. V.; Kopchuk, D. S.; Slepukhin, P. A.; Kozhevnikov, V. N. *Tetrahedron Lett.* **2006**, *47*, 7025–7029.
(31) Kozhevnikov, V. N.; Whitwood, A. C.; Bruce, D. W. *Chem. Commun.* **2007**, 3826–3828.

Scheme 1. Synthesis of Substituted Thienylpyridines[a]

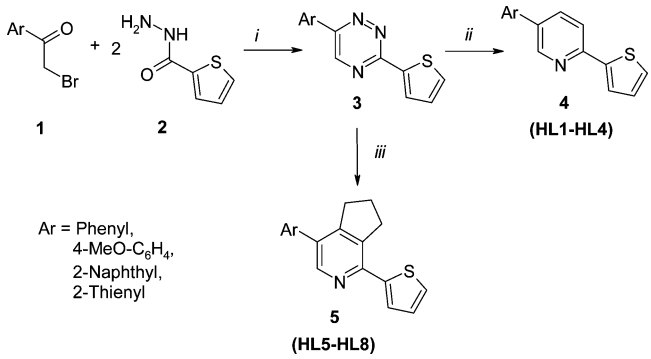

[a] Reagents and conditions: (i) EtOH/AcOH, NaOAc, reflux, 12 h; (ii) 2,5-norbornadiene, *o*-xylene, 200 °C, 12 h; (iii) 1-morpholinocyclopentene, 190 °C, 2 h.

double monochromator. Luminescence decay times of the selectively excited probes were measured using a FAST Comtec (München) multichannel scaler PCI-card with time resolution of 250 ps. For pulsed excitation, a Nd:YAG laser (355 nm, IB Laser Inc., DiNY pQ 02) with a pulse width of 7 ns was applied. All low temperature measurements were carried out with samples of [Pt(L)(acac)] dissolved in *n*-octane (Fluka, p.a. quality) at concentrations of $\approx 10^{-5}$ mol/L.

2.2. Synthesis of Ligands HL1-HL8. General Procedure. 6-Phenyl-3-(2-thienyl)-1,2,4-triazine (**3a**), 6-(4-methoxyphenyl)-3-(2-thienyl)-1,2,4-triazine (**3b**), 6-(2-naphthyl)-3-(2-thienyl)-1,2,4-triazine (**3c**), and 3,6-bis(2-thienyl)-1,2,4-triazine (**3d**) were prepared from the corresponding bromoacetylarenes **1** and (2-thienyl)carboxylic acid hydrazide **2** (see Scheme 1). Mixtures of **1** (10 mmol), **2** (20 mmol), sodium acetate (12 mmol), ethanol (30 mL), and acetic acid (10 mL) were heated under reflux for 12 h. The reaction mixtures were allowed to cool to ambient temperature, and the precipitated solids were filtered off, washed with ethanol, and dried. The obtained products were used for further reactions as obtained, without additional purification.

Ligands HL1-HL4: 5-phenyl-2-(2-thienyl)pyridine (HL1), 5-(4-methoxyphenyl)-2-(2-thienyl)pyridine (HL2), 5-(2-naphthyl)-2-(2-thienyl)pyridine (HL3), and 5,2-bis(2-thienyl)pyridine (HL4) were prepared from the corresponding 2-(2-thienyl)-1,2,4-triazine precursors **3** according to the following procedure. An autoclave equipped with a stirring bar was charged with **3** (1 g), *o*-xylene (10 mL) and norbornadiene (3 mL). The autoclave was sealed, placed in oil bath and heated at 200 °C (oil bath) for 12−24 h. The reaction mixture was filtered through a small pad of silica gel using dichloromethane as eluent. The solvent was removed under reduced pressure, and the residue was triturated with methanol, filtered off, and washed with methanol to give the desired product.

Ligands HL5−HL8: 5-phenyl-2-(2-thienyl)-cyclopenteno[*c*]pyridine (HL5), 5-(4-methoxyphenyl)-2-(2-thienyl)cyclopenteno[*c*]pyridine (HL6), 5-(2-naphthyl)-2-(2-thienyl)cyclopenteno[*c*]pyridine (HL7), and 5,2-bis(2-thienyl)cyclopenteno[*c*]pyridine (HL8) were prepared in reactions of the corresponding 2-(2-thienyl)-1,2,4-triazine precursors **3** with 1-morpholinocyclopentene. Mixtures of the respective 6-aryl-3-(2-thienyl)-1,2,4-triazines (4.0 mmol) and 1-morpholinocyclopentene (3 mL, 18.8 mmol) were stirred at 190 °C under argon atmosphere for 1 h, after which a further portion of 1-morpholinocyclopentene (1 mL, 6.3 mmol) was added and the reaction mixture was still stirred at 190 °C for 1 h. After cooling down to room temperature the reaction mixtures were diluted with dichloromethane and passed through a short silica gel column eluted with dichloromethane. The fractions containing the product were combined, and the solvent was evaporated. The residues were treated with 10 mL of ethanol, upon which solid precipitates formed. The products were separated by filtration and washed with cold ethanol (5 mL).

Characterization. 6-Phenyl-3-(2-thienyl)-1,2,4-triazine (3a). Yield 68%. mp 158−159 °C. ^{1}H NMR (270 MHz, $CDCl_3$): δ 7.21 (dd, 1H, $^3J_{HH}$ 4.8 Hz, $^3J_{HH}$ 3.8 Hz), 7.53−7.60 (m, 4H), 8.08−8.12 (m, 2H), 8.17 (dd, 1H, $^3J_{HH}$ 4.8 Hz, $^4J_{HH}$ 1.2 Hz), 8.95 (s, 1H); ^{13}C NMR (68 MHz, $CDCl_3$): δ 126.5, 128.6, 129.3, 130.9, 131.2, 133.1, 139.5, 146.3, 154.4, 159.9.

6-(4-Methoxyphenyl)-3-(2-thienyl)-1,2,4-triazine (3b). Yield 68%. mp 209−210 °C. ^{1}H NMR (270 MHz, $CDCl_3$): δ 3.85 (s, 3H), 7.15 (m, 2 H), 7.21 (dd, 1H, $^3J_{HH}$ 5.2 Hz, $^3J_{HH}$ 3.7 Hz), 7.89 (dd, 1H, $^3J_{HH}$ 5.2 Hz, $^4J_{HH}$ 1.1 Hz), 8.07 (dd, 1H, $^3J_{HH}$ 3.7 Hz, $^4J_{HH}$ 1.1 Hz), 8.19 (m, 2 H), 9.34 (s, 1H). MS (CI+): *m*/*z* 270 (MH^+).

6-(2-Naphthyl)-3-(2-thienyl)-1,2,4-triazine (3c). Yield 61%. mp 194−195 °C. ^{1}H NMR (270 MHz, $CDCl_3$): δ 7.22 (dd, 1H, $^3J_{HH}$ 5.2 Hz, $^3J_{HH}$ 3.7 Hz), 7.55−7.61 (m, 3H), 7.88−8.03 (m, 3H), 8.19 (dd, 1H, $^3J_{HH}$ 3.7 Hz, $^4J_{HH}$ 1.1 Hz), 8.23 (dd, 1H, $^3J_{HH}$ 8.5 Hz, $^4J_{HH}$ 1.9 Hz), 8.57 (s, 1H), 9.09 (s, 1H). MS (CI+): *m*/*z* 290 (MH^+).

3,6-Bis(2-thienyl)-1,2,4-triazine (3d). Yield 43%. mp 218−219 °C. ^{1}H NMR (270 MHz, $CDCl_3$): δ 7.24 (m, 2H), 7.56 (m, 2H), 7.74 (dd, 1H, $^3J_{HH}$ 3.7 Hz, $^4J_{HH}$ 1.1 Hz), 8.12 (dd, 1H, $^3J_{HH}$ 3.7 Hz, $^4J_{HH}$ 1.1 Hz), 8.86 (s, 1H). MS (EI): *m*/*z* 245 (M^+).

5-Phenyl-2-(2-thienyl)pyridine (HL1). Yield 42%. mp 106−108 °C. ^{1}H NMR (270 MHz, $CDCl_3$): δ 7.12 (dd, 1H, $^3J_{HH}$ 5.0 Hz, $^3J_{HH}$ 3.8 Hz), 7.35−7.52 (m, 4H), 7.58−7.62 (m, 3H), 7.71 (d, 1H, $^3J_{HH}$ 8.4 Hz), 7.87 (dd, 1H, $^3J_{HH}$ 8.4 Hz, $^4J_{HH}$ 2.3 Hz), 8.80 (d, 1H, $^4J_{HH}$ 2.3 Hz). ^{13}C NMR (68 MHz, $CDCl_3$): δ 118.6, 124.5, 126.7, 127.6, 128.0, 128.1, 129.0, 134.6, 134.9, 137.4, 144.5, 147.8, 151.3. Found: C, 76.05; H, 4.78; N, 5.71%. $C_{15}H_{11}NS$ requires: C, 75.91; H, 4.67; N, 5.90%.

5-(4-Methoxyphenyl)-2-(2-thienyl)pyridine (HL2). Yield 34%. mp 154−155 °C. ^{1}H NMR (270 MHz, $CDCl_3$): δ 3.85 (s, 3H), 7.00 (m, 2H), 7.11 (dd, 1H, $^3J_{HH}$ 5.2 Hz, $^3J_{HH}$ 3.7 Hz), 7.38 (dd, 1H, $^3J_{HH}$ 5.2 Hz, $^4J_{HH}$ 1.1 Hz), 7.52 (m, 2H), 7.58 (dd, 1H, $^3J_{HH}$ 3.7 Hz, $^4J_{HH}$ 1.1 Hz), 7.68 (d, 1H, $^3J_{HH}$ 8.2 Hz), 7.83 (dd, 1H, $^3J_{HH}$ 8.2 Hz, $^4J_{HH}$ 2.2 Hz), 8.75 (d, 1H, $^4J_{HH}$ 2.2 Hz). MS (CI+): *m*/*z* 268 (MH^+). Found: C, 72.01; H, 4.99; N, 5.01%. $C_{16}H_{13}NOS$ requires: C, 71.88; H, 4.90; N, 5.24%.

5-(2-Naphthyl)-2-(2-thienyl)pyridine (HL3). Yield 41%. mp 150−151 °C. ^{1}H NMR (270 MHz, $CDCl_3$): δ 7.13 (dd, 1H, $^3J_{HH}$ 5.2 Hz, $^3J_{HH}$ 3.7 Hz), 7.41 (bd, 1H,$^3J_{HH}$ 5.2 Hz), 7.50−7.52 (m, 2H), 7.63 (bd, 1H, $^3J_{HH}$ 3.7 Hz), 7.73−7.77 (m, 2H), 7.89−7.96 (m, 3H), 8.00 (dd, 1H, $^3J_{HH}$ 8.2 Hz, $^4J_{HH}$ 2.2 Hz), 8.04 (bs, 1H), 8.91 (d, 1H, $^4J_{HH}$ 2.2 Hz). MS (CI+): *m*/*z* 288 (MH^+). Found: C, 79.55; H, 4.69; N, 4.78%. $C_{19}H_{13}NS$ requires: C, 79.41; H, 4.56; N, 4.87%.

5,2-Bis(2-thienyl)pyridine (HL4). Yield 66%. mp 153−154 °C. ^{1}H NMR (270 MHz, $CDCl_3$): δ 7.09−7.12 (m, 2H), 7.33−7.36 (m, 2H), 7.39 (bd, 1H, $^3J_{HH}$ 5.2 Hz), 7.58 (bd, 1H, $^3J_{HH}$ 3.9 Hz), 7.65 (d, 1H, $^3J_{HH}$ 8.2 Hz), 7.85 (dd, 1H, $^3J_{HH}$ 8.2 Hz, $^4J_{HH}$ 2.2 Hz), 8.82 (d, 1H, $^4J_{HH}$ 2.2 Hz). MS (CI+): *m*/*z* 244 (M^+). Found: C, 64.31; H, 3.89; N, 5.60%. $C_{13}H_9NS_2$ requires: C, 64.16; H, 3.73; N, 5.76%.

5-Phenyl-2-(2-thienyl)cyclopenteno[c]pyridine (HL5). Yield 82%. mp 128−129 °C. ^{1}H NMR (270 MHz, $CDCl_3$): δ 2.14 (m, 2H, $^3J_{HH}$ 7.6 Hz), 3.04 (t, 2H, $^3J_{HH}$ 7.6 Hz), 3.24 (t, 2H, $^3J_{HH}$ 7.6 Hz), 7.14 (dd, 1H, $^3J_{HH}$ 5.0 Hz, $^3J_{HH}$ 4.0 Hz), 7.34−7.45 (m, 6H), 7.52 (bd, 1H, $^3J_{HH}$ 4.0 Hz), 8.44 (s, 1H). ^{13}C NMR (68 MHz, $CDCl_3$): δ 25.0, 32.6, 33.15, 126.0, 127.2, 127.6, 127.9,

128.43, 128.60, 132.2, 135.2, 137.7, 145.3, 146.8, 147.2, 152.6. Found: C, 78.01; H, 5.58; N, 5.01%. $C_{18}H_{15}NS$ requires: C, 77.94; H, 5.45; N, 5.05%.

5-(4-Methoxyphenyl)-2-(2-thienyl)cyclopenteno[c]pyridine (HL6). Yield 44%. mp 131−132 °C. ^{1}H NMR (270 MHz, $CDCl_3$): δ 2.15 (m, 2H, $^3J_{HH}$ 7.6 Hz), 3.03 (t, 2H, $^3J_{HH}$ 7.6 Hz), 3.24 (t, 2H, $^3J_{HH}$ 7.6 Hz), 3.87 (s, 3H), 6.99 (m, 2H), 7.14 (dd, 1H, $^3J_{HH}$ 5.2 Hz, $^3J_{HH}$ 3.7 Hz), 7.37−7.41 (m, 3H), 7.52 (bd, 1H, $^3J_{HH}$ 3.7 Hz), 8.42 (s, 1H); MS (CI+): *m*/*z* 308 (MH^+). Found: C, 74.39; H, 5.63; N, 4.38%. $C_{19}H_{17}NOS$ requires: C, 74.24; H, 5.57; N, 4.56%.

5-(2-Naphthyl)-2-(2-thienyl)cyclopenteno[c]pyridine (HL7). Yield 55%. mp 145−146 °C. ^{1}H NMR (270 MHz, $CDCl_3$): δ 2.17 (m, 2H, $^3J_{HH}$ 7.6 Hz), 3.10 (t, 2H, $^3J_{HH}$ 7.6 Hz), 3.27 (t, 2H, $^3J_{HH}$ 7.6 Hz), 7.16 (dd, 1H, $^3J_{HH}$ 5.2 Hz, $^3J_{HH}$ 3.7 Hz), 7.42−7.60 (m, 5H), 7.84−7.98 (m, 4H), 8.55 (s, 1H); MS (CI+): *m*/*z* 328 (MH^+). Found: C, 80.57; H, 5.21; N, 4.05%. $C_{22}H_{17}NS$ requires: C, 80.70; H, 5.23; N, 4.28%.

5,2-Bis(2-thienyl)cyclopenteno[c]pyridine (HL8). Yield 65%. mp 137−138 °C. ^{1}H NMR (270 MHz, $CDCl_3$): δ 2.21 (m, 2H, $^3J_{HH}$ 7.6 Hz), 3.18 (t, 2H, $^3J_{HH}$ 7.6 Hz), 3.24 (t, 2H, $^3J_{HH}$ 7.6 Hz), 7.12−7.15 (m, 2H), 7.29 (dd, 1H, $^3J_{HH}$ 3.7 Hz, $^4J_{HH}$ 1.1 Hz), 7.37 (dd, 1H, $^3J_{HH}$ 5.2 Hz, $^4J_{HH}$ 1.1 Hz), 7.41 (dd, 1H, $^3J_{HH}$ 5.2 Hz, $^4J_{HH}$ 0.9 Hz), 7.50 (bd, 1H, $^3J_{HH}$ 3.7 Hz), 8.64 (s, 1H); MS (CI+): *m*/*z* 284 (M^+). Found: C, 67.92; H, 4.68; N, 4.75%. $C_{16}H_{13}NS_2$ requires: C, 67.81; H, 4.62; N, 4.94%.

2.3. Synthesis of [Pt(L)Cl(dmso)] Complexes. General Procedure. To a stirred solution of a cyclometallating agent HL (1 mmol) in acetic acid (30 mL) a solution of potassium tetrachloroplatinate(II) (415 mg, 1 mmol) in water (1 mL) was added. The reaction mixture was heated to 70 °C under nitrogen for 24 h. The chloro-bridged dinuclear intermediate formed in course of the reaction was filtered off, washed with acetic acid (5 mL), ethanol (5 mL), and dried under vacuum. Dimethylsulfoxide (dmso, 2 mL) was then added, and the mixture was heated under reflux for 10 min. Complexes with the cyclometallating ligands which incorporate the cyclopenteno moiety (L5-L8) precipitated upon cooling to room temperature. The precipitates were filtered off and washed with dmso (1 mL) and acetone (3 mL) to give pure compounds. The product complexes with the ligands L1-L4 remained dissolved in dmso. The solvent was removed under reduced pressure, and the residues were dissolved in dichloromethane and purified by column chromatography (silica gel, dichloromethane).

Characterization. [Pt(L1)Cl(dmso)]. Yield 63%. ^{1}H NMR (270 MHz, $CDCl_3$): δ 3.61 (s, 6H, $^3J_{HPt}$ 24.0 Hz, CH_3SOCH_3), 7.21 (m, 5H), 7.60 (m, 3H), 7.96 (dd, 1H, $^3J_{HH}$ 8.4 Hz, $^4J_{HH}$ 2.1 Hz), 9.59 (d, 1H, $^3J_{HH}$ 2.1 Hz, $^3J_{HPt}$ 37.4 Hz). Found: C, 37.48; H, 3.00; N, 2.49%. $C_{17}H_{16}ClNOPtS_2$ requires: C, 37.47; H, 2.96; N, 2.57%.

[Pt(L2)Cl(dmso)]. Yield 71%. ^{1}H NMR (270 MHz, $CDCl_3$): δ 3.61 (s, 6H, $^3J_{HPt}$ 23.5 Hz, CH_3SOCH_3), 3.83 (s, 3H), 6.99 (m, 2H), 7.36 (d, 1H, $^3J_{HH}$ 4.9 Hz), 7.40 (d, 1H, $^3J_{HH}$ 8.4 Hz), 7.52 (m, 2H), 7.62 (d, 1H, $^3J_{HH}$ 4.9 Hz), 7.90 (dd, 1H, $^3J_{HH}$ 8.4 Hz, $^4J_{HH}$ 2.1 Hz), 9.54 (d, 1H, $^3J_{HH}$ 2.1 Hz, $^3J_{HPt}$ 36.2 Hz). Found: C, 37.40; H, 3.32; N, 2.34%. $C_{18}H_{18}ClNO_2PtS_2$ requires: C, 37.60; H, 3.16; N 2.44%.

[Pt(L3)Cl(dmso)]. Yield 58%. ^{1}H NMR (270 MHz, $CDCl_3$): δ 3.63 (s, 6H, $^3J_{HPt}$ 24.5 Hz), 7.37 (d, 1H, $^3J_{HH}$ 4.8 Hz), 7.46−7.53 (m, 3H), 7.64 (bd, 1H, $^3J_{HH}$ 4.8 Hz), 7.69 (dd, 1H,$^3J_{HH}$ 8.5 Hz, $^4J_{HH}$ 1.9 Hz), 7.84−7.89 (m, 2H), 7.93 (d, 1H, $^3J_{HH}$ 8.5 Hz), 8.04 (bs, 1H), 8.08 (dd, 1H, $^3J_{HH}$ 8.9 Hz, $^4J_{HH}$ 2.2 Hz), 9.71 (d, 1H, $^3J_{HH}$ 2.2 Hz, $^3J_{HPt}$ 37.4 Hz). Found: C, 42.49; H, 3.10; N, 2.28%. $C_{21}H_{18}ClNOPtS_2$ requires: C, 42.39; H, 3.05; N, 2.35%.

[Pt(L4)Cl(dmso)]. Yield 52%. ^{1}H NMR (270 MHz, $CDCl_3$): δ 3.61 (s, 6H, $^3J_{HPt}$ 24.1 Hz), 7.10 (dd, 1H, $^3J_{HH}$ 5.2 Hz, $^3J_{HH}$ 3.7 Hz), 7.34−7.39 (m, 4H), 7.61 (d, 1H, $^3J_{HH}$ 5.2 Hz), 7.88 (dd, 1H, $^3J_{HH}$ 8.2 Hz, $^4J_{HH}$ 2.2 Hz), 9.59 (d, 1H, $^3J_{HH}$ 2.2 Hz, $^3J_{HPt}$ 37.4 Hz). MS (EI): *m*/*z* 551 (M^+); 473 ($M^+ - OSC_2H_6$); 436 ($M^+ - OSC_2H_6 - Cl$). Found: C, 32.54; H, 2.70; N, 2.47%. $C_{15}H_{16}ClNOPtS_3$ requires: C, 32.58; H, 2.92; N, 2.53%.

[Pt(L5)Cl(dmso)]. Yield 82%. ^{1}H NMR (270 MHz, $CDCl_3$): δ 2.22 (m, 2H, $^3J_{HH}$ 7.5 Hz), 3.10 (t, 2H, $^3J_{HH}$ 7.5 Hz), 3.15 (t, 2H, $^3J_{HH}$ 7.5 Hz), 3.61 (s, 6H, $^3J_{HPt}$ 24.1 Hz), 7.35−7.50 (m, 5H), 7.71 (d, 1H, $^3J_{HH}$ 5.2 Hz, $^3J_{HPt}$ 18.3 Hz), 9.23 (s, 1H, $^3J_{HH}$ 2.2 Hz, $^3J_{HPt}$ 37.8 Hz). Found: C, 40.90; H, 3.31; N, 2.42%. $C_{20}H_{20}ClNOPtS_2$ requires: C, 41.06; H, 3.45; N, 2.39%.

[Pt(L6)Cl(dmso)]. Yield 74%. ^{1}H NMR (270 MHz, $CDCl_3$): δ 2.21 (m, 2H, $^3J_{HH}$ 7.5 Hz), 3.11 (t, 2H, $^3J_{HH}$ 7.5 Hz), 3.17 (t, 2H, $^3J_{HH}$ 7.5 Hz), 3.60 (s, 6H, $^3J_{HPt}$ 24.0 Hz), 3.85 (s, 3H), 6.96 (m, 2H), 7.35 (m, 2H), 7.45 (d, 1H, $^3J_{HH}$ 5.2 Hz), 7.71 (d, 1H, $^3J_{HH}$ 5.2 Hz), 9.20 (s, 1H, $^3J_{HH}$ 2.2 Hz, $^3J_{HPt}$ 36.5 Hz). Found: C, 40.87; H, 3.81; N, 2.07%. $C_{21}H_{22}ClNO_2PtS_2$ requires: C, 41.01; H, 3.61; N, 2.28%.

[Pt(L7)Cl(dmso)]. Yield 53%. ^{1}H NMR (270 MHz, $CDCl_3$): δ 2.24 (m, 2H, $^3J_{HH}$ 7.6 Hz), 3.18 (t, 2H, $^3J_{HH}$ 7.6 Hz), 3.21 (t, 2H, $^3J_{HH}$ 7.6 Hz), 3.62 (s, 6H, $^3J_{HPt}$ 23.7 Hz), 7.47−7.53 (m, 4H), 7.73 (d, 1H, $^3J_{HH}$ 5.2 Hz, $^3J_{HPt}$ 18.6 Hz), 7.83−7.92 (m, 4H), 9.34 (s, 1H, $^3J_{HPt}$ 36.8 Hz). Found: C, 45.41; H, 3.68; N, 2.13%. $C_{24}H_{22}ClNOPtS_2$ requires: C, 45.39; H, 3.49; N, 2.21%.

[Pt(L8)(dmso)Cl]. Yield 63%. ^{1}H NMR (270 MHz, $CDCl_3$): δ 2.28 (m, 2H, $^3J_{HH}$ 7.6 Hz), 3.17 (t, 2H, $^3J_{HH}$ 7.6 Hz), 3.27 (t, 2H, $^3J_{HH}$ 7.6 Hz), 3.62 (s, 6H, $^3J_{HPt}$ 22.6 Hz), 7.11 (dd, 1H, $^3J_{HH}$ 4.8 Hz, $^3J_{HH}$ 3.7 Hz), 7.32 (dd, 1H, $^3J_{HH}$ 3.7 Hz, $^4J_{HH}$ 1.1 Hz), 7.38 (dd, 1H, $^3J_{HH}$ 4.8 Hz, $^4J_{HH}$ 1.1 Hz), 7.47 (d, 1H, $^3J_{HH}$ 5.2 Hz), 7.70 (d, 1H, $^3J_{HH}$ 5.2 Hz, $^3J_{HPt}$ 18.0 Hz), 9.46 (s, 1H, $^3J_{HPt}$ 37.9 Hz). MS (EI): *m*/*z* 591 (M^+); 513 ($M^+ - OSC_2H_6$). Found: C, 36.52; H, 3.07; N, 2.29%. $C_{18}H_{18}ClNOPtS_3$ requires: C, 36.58; H, 3.07; N, 2.37%.

2.4. Synthesis of [Pt(L)(acac)] Complexes. General Procedure. [Pt(thpy)(acac)] was prepared according to the literature method.[19] Other [Pt(L)(acac)] complexes were prepared from the corresponding [Pt(L)Cl(dmso)] precursors according to the following procedure: A mixture of [Pt(L)Cl(dmso)] (0.1 mmol), sodium acetyl acetonate monohydrate (140 mg, 1.0 mmol) and acetone (10 mL) was stirred at 50 °C for 12 h. Afterward, the reaction mixture was diluted with water (50 mL), and the precipitated solid was filtered off, washed with water, and dried under vacuum.

Characterization. [Pt(L1)(acac)]. Yield 82%. ^{1}H NMR (270 MHz, $CDCl_3$): δ 1.91 (s, 3H), 1.94 (s, 3H), 5.43 (s, 1H), 7.15 (d, 1H, $^3J_{HH}$ 4.8 Hz), 7.21−7.60 (m, 7H), 7.81 (dd, 1H, $^3J_{HH}$ 8.5, Hz, $^4J_{HH}$ 1.9 Hz), 9.00 (d, 1H, $^3J_{HH}$ 1.9, Hz, $^3J_{HPt}$ 41.0 Hz). Found: C, 45.46; H, 3.41; N, 2.56%. $C_{20}H_{17}NO_2PtS$ requires: C, 45.28; H, 3.23; N 2.64%.

[Pt(L2)(acac)]. Yield 76%. ^{1}H NMR (270 MHz, $CDCl_3$): δ 1.96 (s, 3H), 1.99 (s, 3H), 3.85 (s, 3H), 5.47 (s, 1H), 7.00 (m, 2H), 7.18 (d, 1H, $^3J_{HH}$ 4.9 Hz), 7.31 (d, 1H, $^3J_{HH}$ 8.5 Hz), 7.47 (d, 1H, $^3J_{HH}$ 4.9 Hz), 7.50 (m, 2H), 7.82 (dd, 1 H, $^3J_{HH}$ 8.5, Hz, $^4J_{HH}$ 1.9 Hz), 9.00 (d, 1H, $^3J_{HH}$ 1.9, Hz, $^3J_{HPt}$ 43.1 Hz). Found: C, 45.18; H, 3.48; N, 2.37%. $C_{21}H_{19}NO_3PtS$ requires: C, 45.00; H, 3.42; N 2.50%.

[Pt(L3)(acac)]. Yield 90%. ^{1}H NMR (270 MHz, $CDCl_3$): δ 1.97 (s, 3H), 2.00 (s, 3H), 5.49 (s, 1H), 7.21 (d, 1H, $^3J_{HH}$ 4.9 Hz), 7.38 (d, 1H, $^3J_{HH}$ 8.5 Hz), 7.49−7.54 (m, 3H), 7.69 (dd, 1H $^3J_{HH}$ 8.5, Hz, $^4J_{HH}$ 1.9 Hz), 7.85−8.03 (m, 5H), 9.18 (d, 1H, $^3J_{HH}$ 1.9, Hz, $^3J_{HPt}$ 42.1 Hz). MS (EI): *m*/*z* 580 (M^+); 481 (M^+ − acac). Found: C, 49.67; H, 3.43; N, 2.36%. $C_{24}H_{19}NO_2PtS$ requires: C, 49.65; H, 3.30; N 2.41%.

[Pt(L4)(acac)]. Yield 64%. ^{1}H NMR (270 MHz, $CDCl_3$): δ 1.97 (s, 3H), 2.02 (s, 3H), 5.48 (s, 1H), 7.11 (dd, 1H, $^3J_{HH}$ 5.2 Hz, $^3J_{HH}$ 3.7 Hz), 7.18 (d, 1H, $^3J_{HH}$ 4.8 Hz), 7.27 (d, 1H, $^3J_{HH}$ 8.5 Hz),

Table 1. Crystal Data, Data Collection, and Structure Refinement Details for Complexes [Pt(L5)(acac)], [Pt(L6(acac)] and [Pt(L7)(acac)]

	[Pt(L5)(acac)]	[Pt(L6)(acac)]	[Pt(L7)(acac)]
crystal description	platelike	platelike	prism
crystal color	orange-red	orange	orange
empirical formula	$C_{23}H_{21}NO_2PtS$	$C_{24}H_{23}NO_3PtS$	$C_{27}H_{23}NO_2PtS$
formula weight [g mol^{-1}]	570.56	600.58	620.61
crystal size [mm]	0.278/0.226/0.077	0.320/0.220/0.120	0.250/0.130/0.070
crystal system	triclinic	triclinic	Monoclinic
space group	$P\bar{1}$	$P\bar{1}$	$P21/c$
a [Å]	7.3848(3)	7.4727(6)	12.3039(4)
b [Å]	12.2243(5)	11.6062(10)	7.7755(4)
c [Å]	12.2985(4)	12.1314(10)	23.7483(9)
α [deg]	66.667(4)	87.409(10)	90
β [deg]	73.607(3)	83.537(10)	104.809(3)
γ [deg]	76.079(3)	77.083(10)	90
cell volume [Å^3]	967.49(7)	1018.79(15)	2196.51(16)
Z	2	2	4
density [g cm^{-3}]	1.959	1.958	1.877
μ [mm^{-1}]	7.379	7.016	13.038
F(000)	552	584	2416
T [K]	173	123	123
λ [Å]	0.71073	0.71073	1.54184
Θ range [deg]	3.10−32.71	3.59−26.87	3.40−66.65
reflections collected	12996	10536	19857
unique reflections	6371	10536	11569
observed reflections [$I > 2\sigma(I)$]	5386	3849	5467
absorption correction	semiempirical from equivalents	analytical	semiempirical from equivalents
σ_{fin} [e Å^{-3}]	1.768/-1.877	2.264/-0.908	1.496/-1.505
GOF on F^2	0.955	1.068	0.957
final R_1 [$I \geq 2\sigma(I)$]	0.0309	0.0230	0.0347
wR_2	0.0579	0.0568	0.1050

7.31−7.34 (m, 2H), 7.48 (d, 1H, $^3J_{HH}$ 4.8 Hz), 7.83 (dd, 1H, $^3J_{HH}$ 8.5 Hz, $^4J_{HH}$ 2.1 Hz), 9.09 (d, 1H, $^3J_{HH}$ 2.1 Hz,$^3J_{HPt}$ 42.1 Hz). MS (EI): m/z 536 (M^+); 437 (M^+ − acac). Found: C, 40.43; H, 2.97; N, 2.70%. $C_{18}H_{15}NO_2PtS_2$ requires: C, 40.30; H, 2.82; N 2.61%.

[Pt(L5)(acac)]. Yield 54%. ^{1}H NMR (270 MHz, $CDCl_3$): δ 1.95 (s, 3H), 1.97 (s, 3H), 2.21 (m, 2H, $^3J_{HH}$ 7.6 Hz), 3.09 (t, 2H, $^3J_{HH}$ 7.6 Hz), 3.22 (t, 2H, $^3J_{HH}$ 7.6 Hz), 5.46 (s, 1H), 7.26 (d, 1H, $^3J_{HH}$ 4.8 Hz), 7.35−7.50 (m, 5H), 7.58 (d, 1H, $^3J_{HH}$ 4.8 Hz), 8.68 (s, 1H, $^3J_{HPt}$ 37.7 Hz). MS (EI) m/z 571 (MH^+). Found: C, 48.21; H, 3.82; N, 2.31%. $C_{23}H_{21}NO_2PtS$ requires: C, 48.42; H, 3.71; N, 2.45%.

[Pt(L6)(acac)]. Yield 78%. ^{1}H NMR (270 MHz, $CDCl_3$): δ 1.93 (s, 3H), 1.94 (s, 3H), 2.18 (m, 2H, $^3J_{HH}$ 7.6 Hz), 3.05 (t, 2H, $^3J_{HH}$ 7.6 Hz), 3.18 (t, 2H, $^3J_{HH}$ 7.6 Hz), 3.84 (s, 3H), 5.44 (s, 1H), 6.97 (m, 2H), 7.22 (d, 1H, $^3J_{HH}$ 4.8 Hz), 7.35 (m, 2H), 7.54 (d, 1H, $^3J_{HH}$ 4.8 Hz), 8.62 (d, 1H, $^3J_{HH}$ 1.9, Hz, $^3J_{HPt}$ 41.4 Hz). Found: C, 47.93; H, 3.92; N, 2.33%. $C_{24}H_{23}NO_3PtS$ requires: C, 48.00; H, 3.86; N 2.33%.

[Pt(L7)(acac)]. Yield 84%. ^{1}H NMR (270 MHz, $CDCl_3$): δ 1.92 (s, 3H), 1.96 (s, 3H), 2.22 (m, 2H, $^3J_{HH}$ 7.6 Hz), 3.13 (t, 2H, $^3J_{HH}$ 7.6 Hz), 3.23 (t, 2H, $^3J_{HH}$ 7.6 Hz), 5.45 (s, 1H), 7.26 (d, 1H,$^3J_{HH}$ 4.8 Hz), 7.50−7.54 (m, 2H), 7.56 (dd, 1H,$^3J_{HH}$ 8.5 Hz, $^4J_{HH}$ 1.9 Hz), 7.58 (d, 1H,$^3J_{HH}$ 4.8 Hz), 7.87−7.94 (m, 4H), 8.76 (s, 1H, $^3J_{HPt}$ 39.7). MS (EI): m/z 620 (M^+); 521 (M^+ − acac). C, 52.06; H, 3.58; N, 1.98%. $C_{27}H_{23}NO_2PtS$ requires: C, 52.25; H, 3.74; N 2.26%.

[Pt(L8)(acac)]. Yield 78%. ^{1}H NMR (270 MHz, $CDCl_3$): δ 1.97 (s, 3H), 2.00 (s, 3H), 2.27 (m, 2H, $^3J_{HH}$ 7.6 Hz), 3.21 (t, 2H, $^3J_{HH}$ 7.6 Hz), 3.24 (t, 2H, $^3J_{HH}$ 7.6 Hz), 5.48 (s, 1H), 7.13 (dd, 1H, $^3J_{HH}$ 5.2 Hz, $^3J_{HH}$ 3.7 Hz), 7.25 (d, 1H,$^3J_{HH}$ 4.8 Hz), 7.27(dd, 1H, $^3J_{HH}$ 3.7 Hz, $^4J_{HH}$ 1.1 Hz), 7.38 (dd, 1H, $^3J_{HH}$ 5.2 Hz, $^4J_{HH}$ 1.1 Hz), 7.57 (d, 1H, $^3J_{HH}$ 4.8 Hz), 8.89 (s, 1H, $^3J_{HPt}$ 40.6 Hz). MS (EI): m/z 576 (M^+); 477 (M^+ − acac). Found: C, 43.83; H, 3.40; N, 2.37%. $C_{21}H_{19}NO_2PtS_2$ requires: C, 43.74; H, 3.32; N 2.43%.

2.5. X-ray Crystallography. Diffraction data for crystals of [Pt(L6)(acac)] were collected with a STOE-IPDS diffractometer with graphite-monochromated Mo Kα radiation (λ = 0.71073 Å), whereas data for crystals of [Pt(L5)(acac)] and [Pt(L7)(acac)] were collected with an Oxford Diffraction Gemini Ultra CCD diffractometer with Mo Kα (λ = 0.71073 Å) and Cu Kα radiation (λ = 1.5418 Å), respectively. Further crystallographic and refinement data are collected in Table 1. The structures were solved by direct methods (SIR-97)[32] and refined by full-matrix least-squares on F^2 using the SHELXL-97 program.[33] The H atoms were calculated geometrically and a riding model was applied during the refinement process.

3. Results and Discussion

3.1. Syntheses and Structures. The reaction which forms the basis for the synthetic method described below was described first by Saraswathi and Srinivasan in 1971.[34] In this investigation, 2-bromoacetophenone was reacted with 2 equiv of acid hydrazides in the presence of a base to give 3,6-disubstituted-1,2,4-triazines. In our case (compare Scheme 1), the key intermediates, 3-thienyl-1,2,4-triazines **3**, were prepared by reaction of readily available bromoacetylarenes **1** and (2-thienyl)-carboxylic acid hydrazide **2** with the reaction yields varying from 43% to 68%, depending on the nature of the group Ar of the 2-bromoacetophenone derivatives. The next step (*ii* or *iii* in Scheme 1) is the transformation of the triazole

(32) Altomare, A.; Cascarano, G.; Giacovazzo, C.; Guagliardi, A. *J. Appl. Crystallogr.* **1993**, *26*, 343–350.
(33) Sheldrick G. M., *SHELXL-97. Program for crystal structure refinement*; University of Göttingen: Germany, 1997.
(34) Saraswathi, T. V.; Srinivasan, V. R. *Tetrahedron Lett.* **1971**, *12*, 2315–2316.

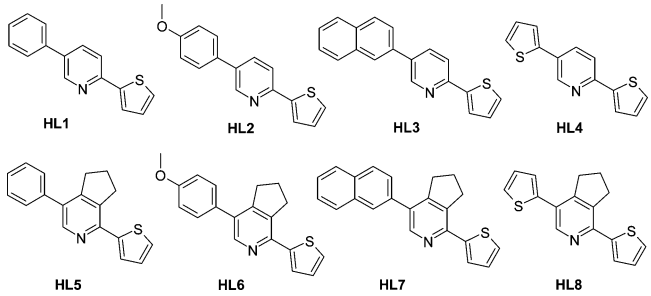

Figure 1. Cyclometallating ligands (protonated) prepared in this study.

derivative into the desired ligand in an inverse-electron-demand Diels−Alder reaction.

Two dienophiles were used in this work: 2,5-norbornadiene (synthetic analogue of acetylene)[35−39] and 1-morpholinocyclopentene (electron-rich enamine)[40−42] which doubles the number of possible structures of the desirable thienylpyridines. Transformations of the triazines **3** to monocyclic pyridines **4** can be performed by heating **3** under reflux with 2,5-norbornadiene in *o*-xylene for 3 to 5 days. Application of an autoclave and elevated temperatures (200 °C) allowed the reactions to complete in a relatively short time (12−24 h) with no adverse effects on the yields (34 to 66%). Reactions of triazines **3** with 1-morpholinocyclopentene proceeded more readily (full conversion was achieved in 2 h) to give cyclopenteno[c]pyridines **5** in 44 to 82% yields. The methodology uses no cross-coupling reactions and therefore expensive reagents and complicated reaction conditions can be avoided in the preparation of such ligands. The method is easily scalable and can be performed on a multigram scale. The chemical structures of all ligands prepared in this study are shown in Figure 1.

According to literature data, reaction of $K_2[PtCl_4]$ with an 2.5 molar excess of a cyclometallating ligand leads to either a dinuclear halogen-bridged complex $[Pt_2(\mu\text{-}Cl)_2L_2]$ (L represents the *ortho*-metallated η^2 ligands) or a mononuclear complex of the formula [Pt(L)(HL)Cl].[19,43,44] We have found that the reactions of $K_2[PtCl_4]$ with 2.5 mol equiv of thienylpyridine derivatives HL1−HL8 in acetic acid lead to mixtures of mononuclear [Pt(L)(HL)Cl] and dinuclear $[Pt_2(\mu\text{-}Cl)_2L_2]$ complexes (Scheme 2). In some cases, the mononuclear complexes were the major products and could be isolated from the reaction mixtures. On the other hand, reaction of $K_2[PtCl_4]$ with equimolar quantities of

Scheme 2. Synthesis of the [Pt(L)(acac)] Complexes[a]

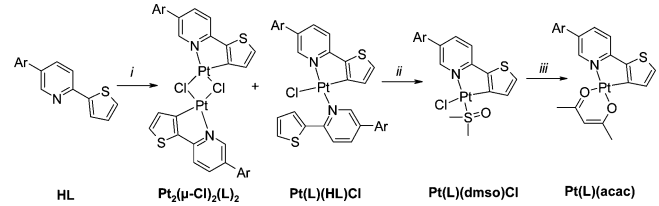

[a] Reagents and conditions: (i) $K_2[PtCl_4]$, acetic acid, reflux, 24 h; (ii) dmso, reflux, 10 min; (iii) [Na(acac)], acetone, room temperature, 12 h.

ligands HL afforded exclusively the very poorly soluble dinuclear complexes $[Pt_2(\mu\text{-}Cl)_2L_2]$. The procedure can be improved by using an aqueous solution of the platinum salt, which shortens the reaction time required to give the dinuclear product. Both mono- and dinuclear complexes can be easily converted into the respective dmso complexes (dmso = dimethylsulfoxide) by heating these complexes (a pure dimeric complex or a mixture of the mono- and dinuclear complexes) in a dimethylsulfoxide, which yields the mononuclear complexes, [Pt(L)Cl(dmso)]. These latter complexes can readily be isolated and purified. A reaction of [Pt(L)Cl(dmso)] with sodium acetyl acetonate, [Na(acac)], in acetone gives the target [Pt(L)(acac)] complexes in high yields. More details concerning the synthetic procedures can be found in our earlier communication (see ref 45).

Crystallization of [Pt(L5)(acac)], [Pt(L6)(acac)], and [Pt(L7)(acac)] via slow diffusion of diethyl ether into concentrated solutions of these complexes in dichloromethane afforded orange to orange-red crystals of sufficient quality for an X-ray structure determination. All of these complexes crystallize in the triclinic $P\bar{1}$ space group. Molecules of all three [Pt(L)(acac)] complexes pack as centrosymmetric head-to-tail dimers and display a square-planar coordination of the Pt-ion, typical for d^8 transition metal complexes.[46,47] Perspective drawings of the [Pt(L5)(acac)], [Pt(L6)(acac)], and [Pt(L7)(acac)] molecules are shown in Figure 2.

In crystals of [Pt(L5)(acac)] and [Pt(L6)(acac)] the molecules are oriented in layer-like structures (Figure 3a). The distance between the planes being about 3.5 Å is indicative of $\pi\pi$ interactions between the aromatic parts of the [Pt(L5)(acac)] and [Pt(L6)(acac)] molecules. There are no direct intermolecular Pt−Pt contacts. The quasi-planar parts of the [Pt(L)(acac)] molecules consisting of the [Pt(acac)] unit and the coordinating part of the cyclometallating ligand L (thiophene and pyridine ring) lie on these planes, whereas the aromatic side-groups attached to the pyridine ring, phenyl in [Pt(L5)(acac)] and 4-methoxyphenyl in [Pt(L6)(acac)], are twisted by 44° and 56°, respectively. In crystals of [Pt(L7)(acac)] the bulkier naphthyl side-groups prevent such an layer-by-layer orientation of the molecules (Figure 3b), which may be a reason for the different macroscopic forms

(35) Pabst, G. R.; Schmid, K.; Sauer, J. *Tetrahedron Lett.* **1998**, *39*, 6691–6694.
(36) Pabst, G. R.; Sauer, J. *Tetrahedron Lett.* **1998**, *39*, 8817–8820.
(37) Pfüller, O. C.; Sauer, J. *Tetrahedron Lett.* **1998**, *39*, 8821–8824.
(38) Pabst, G. R.; Pfüller, O. C.; Sauer, J. *Tetrahedron* **1999**, *55*, 8045–8064.
(39) Kozhevnikov, V. N.; Kozhevnikov, D. N.; Shabunina, O. V.; Rusinov, V. L.; Chupakhin, O. N. *Tetrahedron Lett.* **2005**, *46*, 1521–1523.
(40) Bromley, W. J.; Gibson, M.; Lang, S.; Raw, S. A.; Whitwood, A. C.; Taylor, R. J. K. *Tetrahedron* **2007**, *63*, 6004–6014.
(41) Laphookhieo, S.; Jones, S.; Raw, S. A.; Sainz, Y. F.; Taylor, R. J. K. *Tetrahedron Lett.* **2006**, *47*, 3865–3870.
(42) Kozhevnikov, V. N.; Kozhevnikov, D. N.; Rusinov, V. L.; Chupakhin, O. N.; König, B. *Synthesis* **2003**, *15*, 2400–2405.
(43) Mdleleni, M. M.; Bridgewater, J. S.; Watts, R. J.; Ford, P. C. *Inorg. Chem.* **1995**, *34*, 2334–2342.
(44) Cho, J. Y.; Suponitsky, K. Y.; Li, J.; Timofeeva, T. V.; Barlow, S.; Marder, S. R. *J. Organomet. Chem.* **2005**, *690*, 4090–4093.
(45) Kozhevnikov, V. N.; Ustinova, M. M.; Slepukhin, P. A.; Santoro, A.; Bruce, D. W.; Kozhevnikov, D. N. *Tetrahedron Lett.* **2008**, *49*, 4096–4098.
(46) Breu, J.; Range, K.-J.; von Zelewsky, A.; Yersin, H. *Acta Crystallogr.* **1997**, *C53*, 562–565.
(47) Stückl, A. C.; Klement, U.; Range, K.-J. *Z. Kristallogr.* **1993**, *208*, 297–298.

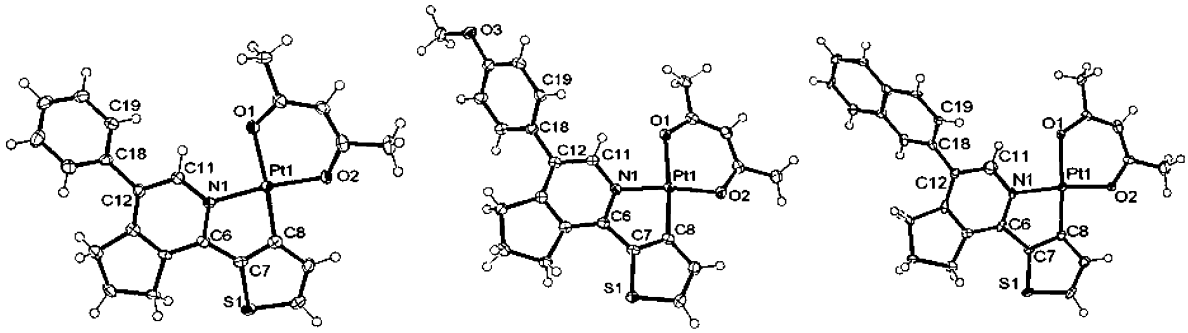

Figure 2. ORTEP drawings of the [Pt(L5)(acac)] (left), [Pt(L6)(acac)] (middle), and [Pt(L7)(acac)] (right) molecules. Selected bond lengths [Å], angles [deg], and torsion angles [deg] are listed in Supporting Information, Table S1.

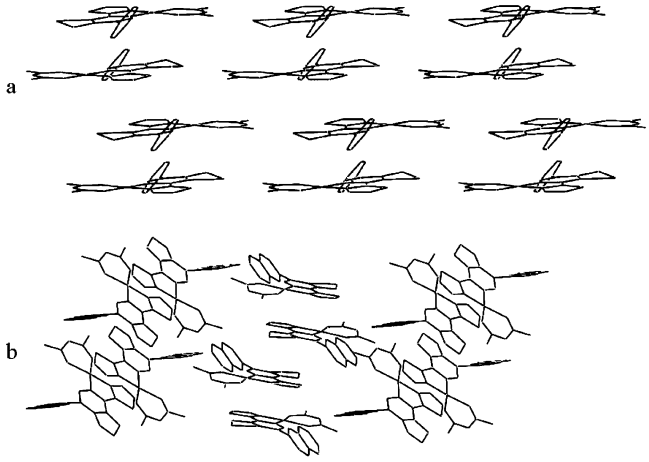

Figure 3. Molecule packing in crystals of [Pt(L5)(acac)] (a) and [Pt(L7)(acac)] (b).

of the crystals: prisms ([Pt(L7)(acac)]) and plates ([Pt(L5)-(acac)] and [Pt(L6)(acac)]; Table 1).

3.2. Photophysical Trends. Figure 4 shows the absorption and luminescence spectra of eight [Pt(L)(acac)] complexes dissolved in dichloromethane and measured at ambient temperature. Table 2 summarizes the data of resolved absorption bands and presents information on the emission behavior, such as positions of luminescence maxima, emission decay times in different solvents/matrixes, as well as luminescence quantum yields.

The absorption spectra of the investigated complexes [Pt(L)(acac)] show similar spectral features as the analogous complex with the unsubstituted thpy ligand [Pt(thpy)(acac)][19]and therefore are assigned equivalently. The high-energy intense absorption bands largely result from excitations from the singlet ground state to singlet excited states of ligand-centered $\pi\pi^*$ character. The low-energy absorption bands with maxima between 420 and 440 nm can be assigned to transitions of mixed metal-to-ligand charge-transfer (MLCT) and $\pi\pi^*$ character. Compared with [Pt(thpy)(acac)] measured under the same experimental conditions (dichloromethane solution, ambient temperature), the lowest absorption bands of the studied [Pt(L)(acac)] complexes are slightly red-shifted. The largest shift of about 1200 cm^{-1} is observed for the complex with the cyclomatallating ligand substituted with the 2-thienyl group, [Pt(L4)(acac)], with $\lambda_{abs} = 445$ nm compared to 422 nm for [Pt(thpy)(acac)].

Similarly, the emission behavior of the studied [Pt(L)-(acac)] complexes strongly resembles that of [Pt(thpy)(acac)]. Degassed dichloromethane solutions of [Pt(L)(acac)] exhibit red photoluminescence, and the emission bands show some resolved vibrational satellite structures even at ambient temperature. The emission decay times lie in the range of several μs, and the emission quantum yields ϕ_{PL} range from 4% for [Pt(L4)(acac)] up to 28% for [Pt(L5)(acac)]. (Table 2) These properties, in particular in combination with the relatively long emission decay times of about 20 μs at 77 K, indicate an assignment of the emitting triplet state as being predominantly of $^3\pi\pi^*$ character.

The data collected in Table 2 show clearly that the photoluminescence properties of the investigated series of [Pt(L)(acac)] depend on the various substituents of the pyridine ring of the cyclometallating ligand L. The emission bands of all [Pt(L)(acac)] complexes studied at $T = 77$ K are red-shifted with respect to [Pt(thpy)(acac)] (with $\lambda_{em} = 553$ nm). The extent of the shift varies from about 400 cm^{-1} in the case of [Pt(L5)(acac)] (with $\lambda_{em} =$ 566 nm) up to 1800 cm^{-1} for [Pt(L4)(acac)] (with $\lambda_{em} =$ 615 nm). Similar trends are also observed at ambient temperature. Since the lowest electronic transition mainly involves an intraligand shift of electron density from the electron-rich thiophene to the electron-deficient pyridine part of the ligand[19] (compare also section 4), the spectral shifts of the emission and the lowest absorption bands might be explainable by the electron donating/withdrawing character of the various substituents. In particular, electron withdrawing substituents at the pyridine part of the ligands L should lower and electron donating substituents should raise the energy of the lowest unnoccupied molecular orbital (LUMO). However, the relatively strong electron donating 4-methoxy and 2-thienyl substituents lead to substantial red shifts of emission and lowest absorption bands. Thus, the above considerations are not suitable to describe the observed energy shifts, especially those induced by these two aromatic side groups. Instead, the stabilizing effects of the investigated aromatic/heteroaromatic substituents on the lowest excited states of the [Pt(L)(acac)] complexes are probably related to an increase of a delocalization of the LUMO involving also the aryl/heteroaryl substituents. In complexes of the series [Pt(L5)(acac)] to [Pt(L8)(acac)], the stabilization of the LUMO energy is smaller because of the cyclopenteno

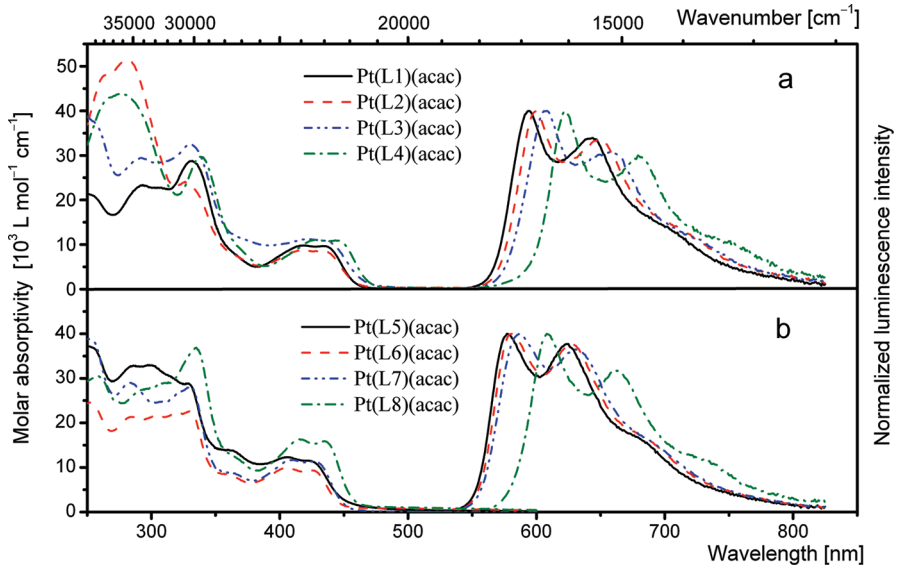

Figure 4. Absorption and luminescence spectra of [Pt(L)(acac)] complexes. All spectra are measured as dichloromethane solutions at ambient temperature. The emission spectra were recorded upon excitation into the lowest absorption band of each compound (λ_{exc} = 410 to 440 nm). The concentration of the [Pt(L)(acac)] complexes was about 10^{-4} mol/L. The absorbances measured at the maximum of the lowest absorption band did not exceed 0.4.

Table 2. Absorption and Luminescence Data of [Pt(L)(acac)] Complexes[a]

	absorption	emission							
	λ_{abs} [nm][b](ε [10^3 L mol^{-1} cm^{-1}])	λ_{em}[c] [nm]	τ[d] [μs]	ϕ_{PL}[e]	λ_{em}[c] [nm]	τ [μs][d]	λ_{em}[c] [nm]	τ [μs][d]	ϕ_{PL}[e,h]
solvent/matrix	dichloromethane	dichloromethane			2-methyl tetrahydrofuran		poly(methyl methacrylate)		
temperature	300 K	300 K			77 K		300 K		
[Pt(thpy)(acac)][f]	422 (2.9), 403 (3.2), 360 (4.6), 331 (10.9), 315 (10.6), 285 (10.8)	558	21	0.42	553	20	558	18	0.45
[Pt(L1)(acac)]	425 (8.7), 328 (23.8), 292 (51.5)	596	13	0.18	581	17	590	14	0.24
[Pt(L2)(acac)]	426 (10.4), 331 (28.7), 294 (22.9)	600	9	0.10	587	14	595	11	0.16
[Pt(L3)(acac)]	430 (11.9), 334 (31.9), 292 (28.2), 255 (35.8)	608	12	0.14	589	18	601	13	0.19
[Pt(L4)(acac)][g]	445 (11.1), 426 (11.2), 340 (30.5), 298 (21.2)	622	6	0.04	615	8	620	6	0.10
[Pt(L5)(acac)][g]	426 (11.5), 405 (12.3), 361 (10.6), 331 (27.4), 302 (26.8), 284 (26.1), 255 (30.5),	577	18	0.28	566	21	576	17	0.35
[Pt(L6)(acac)]	427 (9.3), 406 (9.9), 330 (22.3), 284 (21.4), 252 (24.8)	583	14	0.21	571	19	577	15	0.27
[Pt(L7)(acac)]	419 (11.0), 329 (25.3), 283 (26.7), 254 (35.7),	587	16	0.23	571	21	584	18	0.30
[Pt(L8)(acac)]	435 (15.9), 416 (16.3), 335 (37.0), 290 (31.0), 260 (34.3)	610	8	0.07	591	15	607	10	0.10

[a] Structural formulas of the ligands L1−L8 are shown in Figure 1. [b] λ_{abs} = absorption band maximum, ε = molar absoptivity (experimental error ± 5%). [c] λ_{em} = emission maximum (error ± 1 nm). [d] τ = emission decay time measured after pulsed excitation at λ = 372 nm; experimental error ± 0.5 μs. [e] ϕ_{PL} = photoluminescence quantum yield; experimental error ± 15%. [f] See also ref 19. [g] For detailed spectroscopic investigations, see below. [h] Measured under nitrogen atmosphere.

group, which sterically forces the ligands L5-L8 to adopt a less planar conformation. In addition, the presence of the cyclopenteno goup results in a higher energy of the molecular frontier orbitals because of the electron donating character of this aliphatic group. (For DFT optimized molecular structures of [Pt(L1)(acac)], [Pt(L5)(acac)], [Pt(thpy)(acac)], and [Pt(cyclopenteno-thpy)(acac)] along with contour plots and energies of the corresponding HOMOs and LUMOs see the Supporting Information).

The different substitutions of the cyclometallating ligands L also lead to changes of other excited-state properties, such as emission decay times and photoluminescence quantum yields. (Table 2) The observed changes are related to the spectral shifts discussed above. In particular, the longer the emission wavelengths, the shorter is the emission decay time and the lower the emission quantum yield. Very probably, these effects can be traced back to the growing importance of the non-radiative deactivation according to the energy gap law.[48−51]

3.3. Detailed Characterization of the Emitting Triplet State by High Resolution Luminescence Studies. The nature of the emitting triplet state $\mathbf{T_1}$ of the platinum complexes of the type [Pt(L)(acac)] is not yet sufficiently assigned. In particular, it is not yet clear, whether the $\mathbf{T_1}$ state is of largely mixed ^{3}MLCT-^{3}LC character or, as indicated by the discussions in the preceding section, is rather a ^{3}**LC** ($^3\boldsymbol{\pi\pi^*}$) state.

(48) Caspar, J. V.; Meyer, T. J. *J. Phys. Chem.* **1983**, *87*, 952–957.
(49) Caspar, J. V.; Kober, E. M.; Sullivan, B. P.; Meyer, T. J. *J. Am. Chem. Soc.* **1982**, *104*, 630–632.
(50) Sacksteder, L.; Zipp, A. P.; Brown, E. A.; Streich, J.; Demas, J. N.; DeGraff, B. A. *Inorg. Chem.* **1990**, *29*, 4335–4340.
(51) Stufkens, D. J.; Vlèek, A., Jr. *Coord. Chem. Rev.* **1998**, *177*, 127–179.

In a series of investigations it has been shown that a reliable assignment is obtainable when highly resolved spectra and detailed information on the triplet substates is available (e.g., see refs 52 and 53). Therefore, high-resolution investigations have been carried out for two representative examples, [Pt(L4)(acac)] and [Pt(L5)(acac)].

At first, we will focus on [Pt(L5)(acac)]. For a frozen solution of the complex in *n*-octane at a concentration of $c \approx 10^{-5}$ mol/L (Shpol'skii matrix isolation technique) highly resolved spectra have been obtained. At $T = 4.2$ K and with UV excitation at 375 nm, a manifold of narrow emission lines with half-widths of about 3 cm^{-1} and a broad background can be observed. (See Supporting Information, Figure S1.) The narrow lines result from [Pt(L5)(acac)] molecules (dopants) which substitute two or three matrix molecules of the crystalline host. Since this can occur in different ways, various sites are built at which the dopants experience different interactions with their respective environments. The background comes from inhomogeneously distributed dopants. A similar spectroscopic behavior has been observed for other Pt(II) and also Ir(III) complexes doped into various Shpol'skii or Shpol'skii-like matrixes and explained equivalently (e.g., compare refs 54 and 55). The most intense lines represent electronic 0−0 transitions of the different sites. The distribution of these sites covers a range of about 400 cm^{-1}. The intense line of lowest energy, located at 17199 cm^{-1}, is assigned to site A. This site is well suited for site selective emission and excitation experiments by use of a tunable dye laser, because the absorptions of all other sites lie at higher energies and thus it is possible to excite molecules of this site selectively.

In Figure 5a, a selectively excited emission spectrum of site A measured at $T = 1.2$ K is shown. The dominating peak, lying at 17199 cm^{-1}, is found at the same energy as the dominating peak in the corresponding excitation spectrum. (Figures 5b and 5c) This transition represents the highest energy feature of the low-temperature emission spectrum and the lowest energy feature of the excitation spectrum. Therefore, these peaks are assigned to the electronic 0−0 transition between the lowest triplet state $\mathbf{T_1}$ and the electronic singlet ground state $\mathbf{S_0}$. Apart from the electronic origin line, the emission spectrum shows a number of weaker lines (Figure 5a), which represent vibrational satellites. The satellites up to about 100 cm^{-1} red-shifted relative to the electronic origin have significant lattice or chromophore-cage mode character. Overlapping with this energy range up to $\approx$ 600 cm^{-1}, one usually finds metal−ligand (M−L) vibrations. Fundamentals with energies higher than $\approx$600 cm^{-1} can be classified as ligand vibrations. In this range possibly also M−L progressions and combinations can occur.[52−54]

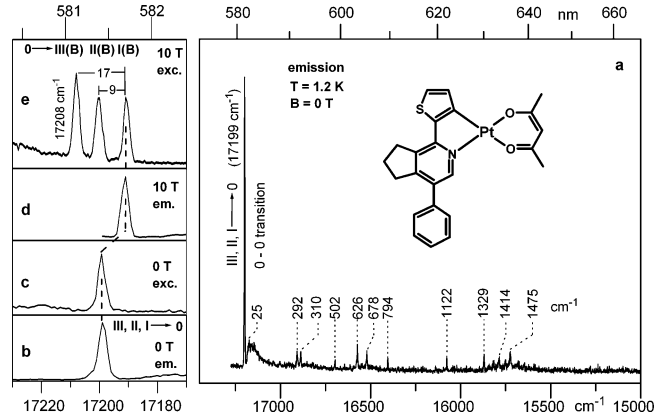

Figure 5. Emission and excitation spectra of site A of [Pt(L5)(acac)] in *n*-octane at a concentration of $c \approx 10^{-5}$ mol/L measured at low temperature and different magnetic fields. The spectrum (a) shows the selectively excited emission of site A excited at λ_{exc}= 17797 cm^{-1} (17199 cm^{-1} + 598 cm^{-1}, vibrational satellite). The spectra (a) and (b) and (c) to (e) were recorded at $T = 1.2$ K and $T = 1.5$ K, respectively. The diagrams at the left-hand side, (b) to (e), show the region of the electronic origins in an enlarged scale: (b) enlarged 0−0 transition line of the emission spectrum (a), (c) excitation spectrum detected at the vibrational satellite at 16573 cm^{-1} (17199−626 cm^{-1}), (d) emission spectrum in the region of the electronic origins at $B = 10$ T at a selective excitation of the substate **III(B)** at 17208 cm^{-1}, and (e) excitation spectrum in the region of the electronic 0−0 transitions to **I(B)**, **II(B)**, and **III(B)** at $B = 10$ T detected at λ_{det} = 16565 cm^{-1} (17191−626 cm^{-1}, vibrational satellite). Note that with the increase of the magnetic field, the detection energy was red-shifted by 8 cm^{-1} to match the energy of the corresponding vibrational satellite at $B = 10$ T.

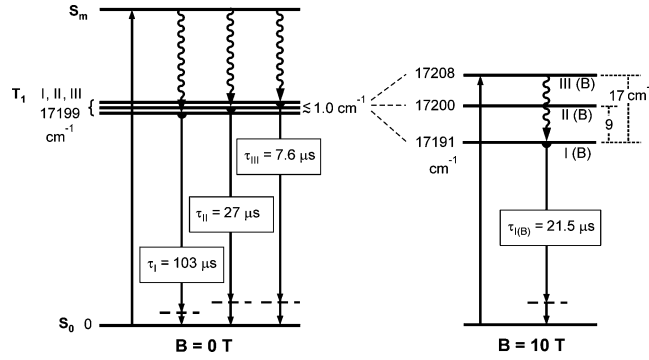

Figure 6. Energy level diagrams and emission decay times for the substates of the lowest triplet state $\mathbf{T_1}$ of [Pt(L5)(acac)] in *n*-octane ($c \approx 10^{-5}$ mol/L) at $B = 0$ T (left) and $B = 10$ T (right). The emission decay times refer to $T = 1.2$ K ($B = 0$ T) and $T = 1.5$ K ($B = 10$ T), respectively. $\mathbf{S_m}$ is a higher lying singlet state.

In organo-transition metal compounds, the triplet term $\mathbf{T_1}$ is very often split into three substates which are separated by several wavenumbers even at zero magnetic field. For [Pt(L5)(acac)], however, at $B = 0$ T only one electronic 0−0 transition is observed with the spectral resolution of our experimental equipment of about 1 cm^{-1}. However, the three substates manifest themselves by their different emission decay times. After a pulsed excitation into a higher lying singlet state ($\lambda_{exc} = 355$ nm, $\tilde{\nu}_{exc} = 28169$ cm^{-1}, pulse width 7 ns) the emission decay is strongly non-monoexponential. The best fit to the experimental decay curve can be obtained with a tri-exponential decay function. This leads to three components of $\tau_I = (103 \pm 5)$ μs, $\tau_{II} = (27 \pm 3)$ μs, and $\tau_{III} = (7.6 \pm 1)$ μs (see also Figure 6) with relative contributions of the integrated emissions of 6, 22, and 72%, respectively. For $T \geq 50$ K, the decay becomes monoexponential with a

(52) Yersin, H.; Donges, D. *Top. Curr. Chem.* **2001**, *214*, 81–186.
(53) Yersin, H.; Finkenzeller, W. J. In *Highly Efficient OLEDs with Phosphorescent Materials*; Yersin, H., Ed.; Wiley-VCH: Weinheim, 2008; pp 1−97.
(54) Wiedenhofer, H.; Schützenmeier, S.; von Zelewsky, A.; Yersin, H. *J. Phys. Chem.* **1995**, *99*, 13385–13391.
(55) Finkenzeller, W. J.; Hofbeck, T.; Thompson, M. E.; Yersin, H. *Inorg. Chem.* **2007**, *46*, 5076–5083.

decay time of $\tau = 20\ \mu s$ (measured at $T = 52$ K). This behavior can be explained as follows: The energy splitting of the triplet term into three substates is about or less than 1 cm^{-1}. After UV excitation, these substates are populated individually because of individual and fast intersystem crossing processes.[56] At $T = 1.2$ K, these $\mathbf{T_1}$ sublevels are not in a thermal equilibrium because the relaxation rates between them are very small due to very slow processes of spin−lattice relaxation (SLR) at small energy separations between the triplet substates.[52,56−58] Therefore, all three sublevels emit according to their individual decay times. With temperature increase, for example, to $T \geq 50$ K, the processes of SLR become faster than the individual decay times of the substates of $\mathbf{T_1}$. As consequence, the luminescence decay becomes monoexponential with an average emission lifetime of 20 μs. According to detailed investigations of the temperature dependence of the emission decay behavior carried out with $[Pd(thpy)_2]$,[52,59] the relevant SLR process is assigned to a Raman process. Similar behavior has also been observed for $[Pt(qol)_2]$ (with qol = 8-hydroxyquinolinate),[56] $[Ir(ppy)_2(CO)Cl]$ (with ppy = 2-phenylpyridine),[60] and $[Re(pbt)(CO)_4]$ (with pbt = 2-phenylbenzothiazole).[61]

The existence of three close-lying triplet sublevels can further be substantiated by application of high magnetic fields. With an increase of the magnetic field strength, the 0−0 line at 17199 cm^{-1} ($\mathbf{S_0} \rightarrow \mathbf{T_1}$) splits into three Zeeman lines (Figure 5e) because of the magnetic field induced mixings of the corresponding wave functions.[59,62] At $B =$ 10 T, the splittings between the B-field disturbed substates **I(B)** and **II(B)**, and **I(B)** and **III(B)** amount to $\Delta E_{I,II}(B =$ 10 T) = 9 cm^{-1} and $\Delta E_{I,III}(B = 10$ T) = 17 cm^{-1}, respectively. This observation represents also a clear confirmation of the triplet nature of the corresponding state. Detailed energy level diagrams for [Pt(L5)(acac)] at $B = 0$ T and B = 10 T are depicted in Figure 6.

Application of high magnetic fields strongly influences the emission decay behavior of the $\mathbf{T_1}$ excited state. With increasing B-field, the emission decay time of substate **I** decreases from $\tau_I = 103\ \mu s$ ($T = 1.2$ K, $B = 0$ T) to $\tau_{I(B)} =$ 21.5 μs ($T = 1.5$ K, $B = 10$ T). This behavior is a consequence of the B-field induced mixings of substate **I** with the shorter living substates **II** and **III**. At high field, the decay becomes monoexponential because of the fast thermal equilibration according to the increasing importance of the direct processes of SLR[57] at larger splitting energies between the $\mathbf{T_1}$ substates. The Zeeman effects as described above are typical for three substates of one parent $\mathbf{T_1}$ term.[55−57,61]

(56) Donges, D.; Nagle, J. K.; Yersin, H. *Inorg. Chem.* **1997**, *36*, 3040–3048.
(57) Yersin, H.; Strasser, J. *Coord. Chem. Rev.* **2000**, *208*, 331–364.
(58) Yersin, H.; Donges, D.; Nagle, J. K.; Sitters, R.; Glasbeek, M. *Inorg. Chem.* **2000**, *39*, 770–777.
(59) Schmidt, J.; Wiedenhofer, H.; von Zelevsky, A.; Yersin, H. *J. Phys. Chem.* **1995**, *99*, 226–229.
(60) Finkenzeller, W. J.; Stoessel, P.; Yersin, H. *Chem. Phys. Lett.* **2004**, *397*, 289–295.
(61) Czerwieniec, R.; Finkenzeller, W. J.; Hofbeck, T.; Starukhin, A.; Wedel, A.; Yersin, H. *Chem. Phys. Lett.* **2009**, *468*, 205–210.
(62) Azumi, T.; O'Donnell, C. M.; McGlynn, S. P. *J. Chem. Phys.* **1966**, *45*, 2735–2742.

Table 3. Energies of the Emitting $\mathbf{T_1}$ State, Emission Decay Times, Zero-Field and B-field Induced ($B = 10$ T) Splittings of $\mathbf{T_1}$ State in [Pt(L4)(acac)] and [Pt(L5)(acac)][a]

	[Pt(L4)(acac)]	[Pt(L5)(acac)]
$\mathbf{T_1} \leftrightarrow \mathbf{S_0}$ 0−0 transition	16150 cm^{-1}	17199 cm^{-1}
τ_I[b]	≈ 27 μs[c]	103 μs
τ_{II}[b]	≈ 27 μs[c]	27 μs
τ_{III}[b]	4 μs[c]	8 μs
τ (77 K)	9 μs	20 μs
ΔE(ZFS)	≤1 cm^{-1}	≤1 cm^{-1}
$\Delta E_{I,III}$(10 T)	17 cm^{-1}	17 cm^{-1}
τ (10 T, 1.5 K)	8.5 μs	21.5 μs

[a] In *n*-octane at a concentration of $c \approx 10^{-5}$ mol/L. [b] Determined at $T =$ 1.2 K. [c] For [Pt(L4)(acac)], a biexponential luminescence decay is observed. The 0−0 line splitting pattern under external magnetic fields and the result that the mean decay time of $\tau_{therm} = 9.3\ \mu s$ − calculated according to $\tau_{therm} = 3/(1/\tau_I + 1/\tau_{II} + 1/\tau_{III})$[59,60] − is nearly equal to the measured decay time of $\tau = 9\ \mu s$ (at $T = 77$ K) lead to the given assignment of $\tau_I \approx \tau_{II} = 27\ \mu s$ and $\tau_{III} = 4\ \mu s$. (Details will be published elsewhere).

With respect to emission wavelengths, decay times, and quantum yields, [Pt(L5)(acac)] shows obvious differences from [Pt(L4)(acac)]. (Table 2) Therefore, we have chosen [Pt(L4)(acac)] as a second candidate for the detailed studies. Table 3 summarizes a series of results. In particular, the electronic 0−0 transition to the lowest excited-state is about 10^3 cm^{-1} lower for [Pt(L4)(acac)] than for [Pt(L5)(acac)], as found for the specific sites in *n*-octane. This is a result of the combined delocalization and donor/acceptor effects induced by the different substituents. (Compare section 3.2.) The significantly shorter emission decay time of the substate **I** of [Pt(L4)-(acac)] compared to that of [Pt(L5)(acac)] is presumably a consequence of a slightly stronger spin−orbit coupling to higher lying singlet states. However, the zero-field splittings of the $\mathbf{T_1}$ state for the both complexes are similarly smaller than about 1 cm^{-1} and the splittings induced by external magnetic field have at $B = 10$ T the same magnitude of $\Delta E_{I,III}(10\ T) \approx 17\ cm^{-1}$.

In summary, the emitting states of both compounds, and most probably of all complexes of the investigated series exhibit very small splittings of the $\mathbf{T_1}$ states. It will be shown in the next section that in particular the very small splitting of the $\mathbf{T_1}$ state allows us to assign these excited states as being largely of ^{3}**LC** ($^3\pi\pi^*$) character.

4. Assignments and Conclusions

A new efficient and straightforward methodology for the synthesis of cyclometallating ligands, derivatives of 2-(2-thienyl)pyridine, has been demonstrated. A wide variety of the ligands substituted on the pyridine fragment can readily be accessed via triazine intermediates. The different substitutions influence photophysical properties of the [Pt(L)(acac)] complexes by shifting the energy of the lowest excited-state and changing emission decay times and quantum yields. A moderate fine-tuning of the excited-state properties by a judicious choice of the chemical modifications of the cyclometallating ligand seems to be possible. Detailed photophysical investigations carried out for two representative examples, [Pt(L4)(acac)] and [Pt(L5)(acac)], indicate a predominantly ligand centered $^3\pi\pi^*$ character of the emitting triplet state.

The magnitude of the ZFS of the lowest triplet state represents a characteristic value, which can be used to classify the $\mathbf{T_1}$ state with respect to its orbital origin. Such a splitting generally requires d-orbital involvements in the excited state, since only the d-orbital contribution provides mixing paths for spin−orbit coupling (SOC) of the individual triplet sublevels with higher lying triplet and singlet excited states.[53,63−65] Consequently, ZFS displays the extent of the MLCT character of the emitting state $\mathbf{T_1}$.[52,53,57,66] A ZFS-based empirical ordering scheme developed recently for organo-transition metal compounds[52,57,63,66] provides a useful scale for the assessment of the MLCT contribution in the $\mathbf{T_1}$ emitting state. In particular, it was found that high ZFS values, for example, ZFS $\geq$ 50 cm^{-1}, are indicative of a predominantly MLCT character, whereas ZFS values in the range of only a few cm^{-1} or lower point to a predominantly ligand-centered character of the emitting triplet state. Therefore, on the basis of ZFS values found to be $\leq$1 cm^{-1} the lowest excited triplet states of [Pt(L4)(acac)] and [Pt(L5)(acac)] can be assigned as ^{3}**LC**($^3\pi\pi^*$) with only small ^{1,3}**MLCT** admixtures.[52,53,61,66] This assignment is most probably also valid for all [Pt(L)(acac)] complexes investigated in this work. For completeness, it is mentioned that other complexes involving the Pt(thpy) fragment can exhibit significantly larger ZFS values. For example, for [Pt(thpy)Cl(CO)][67] and [Pt(thpy)$_2$][52,54] splittings of 3.8 cm^{-1} and 16 cm^{-1}, respectively, were observed. These results show that the MLCT character of the emitting state or the effectiveness of spin−orbit coupling depends on the chromophoric, as well as on the anilliary, ligand. (Compare ref 68).

It is remarked that the triplet state of an emitter for applications in OLEDs should exhibit a distinct MLCT character. This is required, since the emitter should have a short emission decay time and a high luminescence quantum yield. The requirement of a short emission decay time is particularly crucial for reduction of saturation and triplet−triplet annihilation effects to minimize the roll-off of the device efficiency at high current densities.[69,70] Therefore, complexes of the type [Pt(L)(acac)] do not seem to be the first choice emitters for OLEDs, at least when high brightness is required. This, however, does not exclude possible applications as moderate OLED emitters or as sensors and bioimaging materials.

Acknowledgment. The authors thank the Bundesministerium für Bildung and Forschung, BMBF (R.C., T.F., and H.Y.), the Russian Foundation for Basic Research, RFBR, the University of York (M.M.U and A.S.), the Royal Society (D.N.K), the EU and the EPSRC (V.N.K.) for the funding and Johnson Matthey for generous loans of platinum metal salts.

Supporting Information Available: Selected bond lengths, angles, and dihedral angles of [Pt(L5)(acac)], [Pt(L6)(acac)], and [Pt(L7)(acac)], photoluminescence spectrum of [Pt(L5)(acac)] measured in *n*-octane at 4.2 K under a nonselective excitation at λ_{exc} = 375 nm, results of DFT computations, and crystallographic data in CIF format. This material is available free of charge via the Internet at http://pubs.acs.org.

IC802401J

(63) Rausch, A. F.; Homeier, H. H. H.; Djurovich, P. I.; Thompson, M. E.; Yersin, H. *Proc. SPIE* **2007**, *665*566550F (1−16).
(64) Nozaki, K. *J. Chin. Chem. Soc.* **2006**, *53*, 101–112.
(65) Ikeda, S.; Yamamoto, S.; Nozaki, K.; Ikeyama, T.; Azumi, T.; Burt, J. A.; Crosby, G. A. *J. Phys. Chem.* **1991**, *95*, 8538–8541.
(66) Yersin, H. *Top. Curr. Chem.* **2004**, *241*, 1–26.
(67) Yersin, H.; Donges, D.; Humbs, W.; Strasser, J.; Sitters, R.; Glasbeek, M. *Inorg. Chem.* **2002**, *41*, 4915–4922.
(68) Rausch, A. F.; Thompson, M. E.; Yersin, H. *J. Phys. Chem. A* **2009**, in press.
(69) Giebink, N. C.; Forrest, S. R. *Phys. Rev. B* **2008**, *77*, 235215.
(70) Reineke, S.; Waltzer, K.; Leo, K. *Phys. Rev. B* **2007**, *75*, 125328.